Received: 1 December 2022 | Accepted: 21 November 2023

DOI: 10.1111/2041-210X.14292

Methods in Ecology and Evolution

RESEARCH ARTICLE

LC-ICP-MS analysis of inositol phosphate isomers in soil offers improved sensitivity and fine-scale mapping of inositol phosphate distribution

Joseph J. Carroll[1] | Colleen Sprigg[1] | Graham Chilvers[2] | Ignacio Delso[3] | Megan Barker[4] | Filipa Cox[4] | David Johnson[4] | Charles A. Brearley[1]

[1]School of Biological Sciences, University of East Anglia, Norwich Research Park, Norwich, UK

[2]Science Analytical Facility, University of East Anglia, Norwich Research Park, Norwich, UK

[3]School of Pharmacy, University of East Anglia, Norwich Research Park, Norwich, UK

[4]Department of Earth and Environmental Sciences, University of Manchester, Manchester, UK

Correspondence
Charles A. Brearley
Email: c.brearley@uea.ac.uk

Funding information
Natural Environment Research Council, Grant/Award Number: NE/W000350/1; Biotechnology and Biological Sciences Research Council, Grant/Award Number: BB/M011216/1

Handling Editor: Huijie Qiao

Abstract

1. Organic forms of phosphorus (P) prevail in soils and their quantification is vital to better understand global biogeochemical cycles. P speciation in soil is commonly assessed by ^{31}P NMR spectroscopy of sodium hydroxide-EDTA (NaOH-EDTA) extracts.
2. A liquid chromatography-inductively coupled plasma-mass spectrometry (LC-ICP-MS) method that employs NaOH-EDTA is described.
3. Comparison with 31P NMR shows that LC-ICP-MS is up to three orders of magnitude more sensitive. It allows measurement in samples as small as 1 mg. We reveal variation of inositol phosphate distribution in Swedish boreal forest soil and identify *myo*- and *scyllo*-inositol hexakisphosphates and other isomers including *scyllo*-inositol pentakisphosphate.
4. Speciation of the major inositol phosphates was not altered by long-term nitrogen fertilization.

KEYWORDS
inositol phosphate isomers, LC-ICP-MS, nitrogen fertilization, phosphorus speciation, phytate, soil 31P NMR

1 | INTRODUCTION

Phosphorus (P) is a major nutrient that limits plant growth in diverse ecosystems, including tropical forests (Cunha et al., 2022), boreal forest (Giesler et al., 2012) and species-rich calcareous grassland (Johnson et al., 1999). Sustained input of nitrogen (N) from atmospheric deposition or fertilization increases P limitation of ecosystems globally (Chen et al., 2020) and often results in increased activity of enzymes implicated in organic P degradation (Johnson et al., 2005; Papanikolaou et al., 2010). The chemical diversity of soil P is vast, and resolving the various components of this, especially organic P, is vital to better understand biogeochemical cycling and ecological processes, such as coexistence and dominance of plants in communities (Turner, 2008).

^{31}P NMR spectroscopy of sodium hydroxide-EDTA (NaOH-EDTA) extracts has allowed an analysis of P speciation in soil (Cade-Menun et al., 2002; Doolette et al., 2010; Newman & Tate, 1980; Reusser, Verel, Zindel, et al., 2020). The approach has the advantage of being able to quantify and assign P by speciation (Giles et al., 2011; Jarosch et al., 2015). Even so, assignment of resonances and identification of

form of P within complex NMR spectra presented by soil matrices is most powerful when it is combined with spiking of extracts (Doolette et al., 2009; Liu et al., 2014; McLaren et al., 2022). This approach has been used widely to measure inositol phosphates, reported to be a major form of organic P in many soils (Giles et al., 2011; Turner et al., 2002) or undetectable in others (Doolette et al., 2010).

Despite the benefits, there are limitations to the application of ^{31}P NMR to soils. A contemporary issue is deconvolution of overlapping resonances and their isolation from underlying features (Doolette & Smernik, 2015; Jarosch et al., 2015; McLaren et al., 2015; Reusser, Verel, Frossard, et al., 2020). An alternative approach involves the removal of the so-called humic substances (Doolette et al., 2011; Gerke, 2010) by hypobromite oxidation (Irving & Cosgrove, 1981; Reusser, Verel, Zindel, et al., 2020; Turner et al., 2012). An alternative to chemical 'clean-up' is chromatographic separation, ideally compatible with NaOH-EDTA extractions (Cade-Menun & Preston, 1996) accepted as the most exhaustive extractant of inositol phosphate from soil matrices.

Here, we describe chromatographic separation and quantification of *myo*-, *scyllo*-, *neo*- and *chiro*-inositol hexakisphosphate isomers, besides 'lower' inositol phosphates, by direct analysis of NaOH-EDTA extracts on chromatography interfaced with inductively coupled plasma-mass spectrometry (ICP-MS). The approach is an extension of earlier ICP-MS work (Rugova et al., 2014), employing the considerable resolving power of anion chromatography on acid gradients for resolution of inositol hexakisphosphates (Whitfield et al., 2018). We use the method to characterize inositol phosphates of forest soils that have been fertilized for 38 years with N, as NH_4NO_3, and test the hypothesis that N addition leads to a reduction in inositol phosphate pools.

2 | MATERIALS AND METHODS

2.1 | Soil information

Soils were collected from an 87-year-old *Pinus sylvestris* forest stand in Åsele, Sweden (64°07′ N, 17°33′ E). The site is located 330 m above sea level. The soils are Podzols with a sandy sediment texture. The forest consists of six replicate $30 \times 30\,m^2$ experimental plots, of which three have remained unfertilized and three have been subjected to N fertilization for 38 years at an equivalent to 75 kg N ha^{-1} $year^{-1}$ in the form of NH_4NO_3 (Jacobson & Pettersson, 2010).

2.2 | Soil sampling

From each of the six plots, hereafter 1–6, of which 1–3 were control plots and 4–6 were N-fertilized plots, samples were taken from three areas, hereafter subplot A–C, giving rise to 18 separate samples—nine unfertilized (1A–3C) and nine N-fertilized (4A–6C). Samples were stored at −20°C until processing. Soils taken for analysis of the properties shown in Table S1 were collected to a depth of 10 cm from 15 separate locations within each experimental plot, giving a total of 90 samples across all plots.

2.3 | Properties of the soils used in this study

Soil moisture was calculated by gravimetric weight. Organic content was determined by percentage loss on ignition at 450°C. Water extractable N, also known as dissolved organic N (DON), and water extractable inorganic N, also known as mineral or dissolved inorganic (plant available) N (DIN), were extracted from fresh soils (Bardgett et al., 2007) and analysed using a Seal AA3 flow multi-chemistry auto-analyser (Seal Analytical, UK). Dissolved organic and inorganic C (DOC, DIC) were extracted similarly and analysed on a 5000A TOC analyser (Shimadzu, Japan). Microbial C and N were extracted by fumigation–extraction (Vance et al., 1987) and analysed as above. Total C and N (%) were determined by combustion analysis of oven-dried soils using Vario EL Cube (Elementar, Hanau, Germany). Organic and inorganic P were extracted from dry soils and analysed by treating samples with the ascorbic acid method adapted from Kuo (1996), measuring absorbance at 880 nm with a CLARIOstar microplate reader (BMG Labtech, Ortenberg, Germany).

2.4 | NaOH-EDTA extraction

Samples (0.5 g) of each soil were weighed into a 50-mL Falcon tube in which 5 mL of 0.25 M NaOH/0.05 M EDTA was added. Samples were shaken overnight (~16 h) at 180 rpm at room temperature. One millilitre from each sample was filtered into sampling vials using a 0.22-μm filter.

2.5 | NaOH-EDTA extraction of Arabidopsis seed

Single seeds of Arabidopsis were ground by hand with a plastic pestle in 0.1 mL of 0.25 M NaOH/0.05 M EDTA in a 1.5-mL microfuge tube and incubated overnight at room temperature before centrifugation at 22,000×*g* for 15 min at 4°C. An aliquot of the supernatant (80 μL) was removed to a Chromacol 03-FISV(A) glass autosampler vial.

2.6 | Microfractionation of soil

Replicate samples of 10 mg of soil (Sample 4A of Figure 1) were weighed into microfuge tubes. Separately, 2 g of the same soil was ground and sieved through a 1.4-mm stainless steel sieve. From this, replicate 10-mg portions were taken. All samples/portions were extracted with 100 μL of 0.25 M NaOH/0.05 M EDTA with shaking overnight before centrifugation at 22,000×*g* for 15 min at 4°C. An aliquot of the supernatant (80 μL) was removed to an autosampler vial.

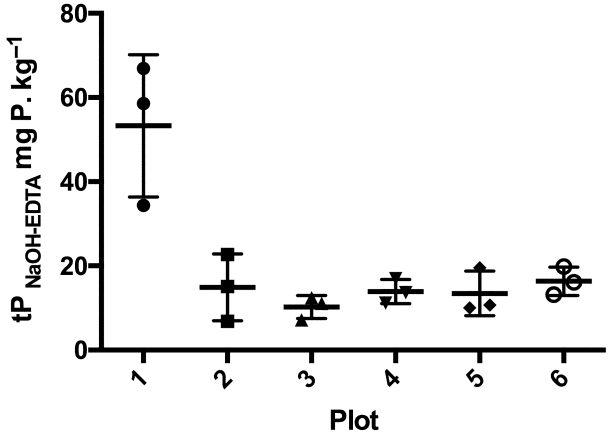

FIGURE 1 NaOH-EDTA-extractable total P ($tP_{NaOH\text{-}EDTA}$), measured by ICP-AES. Fresh soil extracted with NaOH-EDTA at 1:10 mass:volume ratio was diluted and analysed by ICP-AES.

2.7 | ICP-AES analysis of total phosphorus in NaOH-EDTA extracts

NaOH-extracted soil samples were diluted 50-fold in 18.2 mOhm cm water and were compared with single element calibration standards of phosphorus at 2, 4, 6, 8 and 10 ppm, prepared from a 1000-ppm standard (Centi-prep), on a Thermo Icap-Pro Dual view inductively coupled plasma atomic emission spectrometer (ICP-AES). The instrument parameters were: observation direction, radial; wavelength, 178.284 nm; RF power, 1.150 KW; auxiliary gas flow rate, 0.5 L min^{-1}; nebulizer flow rate, 0.5 L min^{-1}; plasma flow rate, 12.5 L min^{-1}; with gas, argon. CertiPrep Multi-Element Solutions 2A and 4 (*Trace*CERT®) were used as independent standards.

2.8 | LC-ICP-MS analysis of inositol phosphates

Samples, typically 10 µL or 100 µL, were analysed on a Dionex™ CarboPac™ PA200 column eluted with HCl (Whitfield et al., 2018) into the PFA concentric nebulizer of a Thermo Icap-TQ (Thermo Scientific) triple quadrupole inductively coupled plasma-mass spectrometer (ICP-MS) used as detector. The iCAP-TQ was tuned prior to the initial sample injection, using a Thermo tune solution (BRE00009578) for Ba, Bi, Ce, Co, Ho, In, Li, Mg, Ti (all 1.0 mg L^{-1} in 2% HNO_3 + 0.5% HCl). The ratio of oxides (CeO/Ce) was maintained at <2% and doubly charged ions ($^{140}Ce^{2+}$ and $^{137}Ba^{2+}$) at 3%. Instrument operating parameters are described in Table 1.

2.9 | Calibration

Influence of LC solvent on detector response to PO^+ at m/z 47 and P^+ at m/z 31 was tested in a matrix of KH_2PO_4 versus HCl delivered at 0.4 mL min^{-1} (Table S2). Response to KH_2PO_4 differed by ≤7% at the concentrations and flow rates used. Analyses were also made following chromatographic separation of inositol phosphates with the column eluate directed in toto to the nebulizer. A calibration curve for injections of *myo*-$InsP_6$ is shown (Figure S1).

TABLE 1 Optimized instrumental parameters for LC-ICP-MS/MS.

Detection standard mode (31P, 31P.16O)	
Instrument	Thermo iCAP-TQ
Plasma RF power	1550 W
Nebulizer gas flow	1.07 L min^{-1}
Auxiliary gas flow	0.796 L min^{-1}
Cool gas flow	14.04 L min^{-1}
Dwell time	0.2 ms
Peristaltic pump speed	40 rpm
Carrier gas	Argon
Reaction gas	Oxygen, O_2

2.10 | ^{31}P NMR spectrum acquisition and processing

NMR spectra were recorded, at 500 MHz for ^1H, with a Bruker AVANCE NEO spectrometer equipped with a 5-mm solution-state iProbe probe-head. Spectra were recorded at ^{31}P frequency of 202.12 MHz, with inverse gated decoupling sequence, applying ^{31}P 90° pulses (P1 calibrated for a length of 12 µs), with a recovery time (D1) of 30 s, a spectral width of 40 ppm centred in 5 ppm (covering the region from 25 to −15 ppm) and an optimized acquisition time of 0.4 s. The number of scans was set to 8192. Spectra were processed with Topspin 4.1.3 by applying an exponential window function with a line-broadening factor of 1 Hz before the Fourier transform to 32 K points. Phase and baseline correction were corrected with the automatic combined phase and baseline algorithm. Methylene diphosphonate (MDP) signal was used as chemical shift reference, set at 16.6 ppm.

3 | RESULTS

3.1 | Soil parameters

The soil parameters measured are shown in Table S1. Content of total P (tP) ranged from 171 to 1009 mg kg^{-1} dry wt with a median of 446 mg kg^{-1}. Of this, inorganic P (IP) ranged from 18 to 817 mg kg^{-1} dry wt with a median of 115 mg kg^{-1} and organic P (OP) ranged from 0 to 840 mg kg^{-1} dry wt with a median of 283 mg kg^{-1}.

Separate samples of soils from the same experimental plots, but not represented in the measurements of Table S1, were analysed for NaOH-EDTA-extractable total phosphorus $tP_{NaOH\text{-}EDTA}$ by ICP-AES at the University of East Anglia (Figure 1).

Total P measured by ICP-AES in NaOH-EDTA-extracted samples fell in the range 6.85 mg P. kg^{-1} measured in subplot 2C to 66.9 mg

P. kg^{-1} in subplot 1B. Mean total P was 20.35 mg P. kg^{-1} across all six plots.

Analysis by one-way ANOVA found significant differences in mean total P between plots ($F_{5,12}=11.8$, $p=0.0003$), with post hoc Tukey's comparison finding Plot 1 to contain significantly higher total phosphorus compared to all other plots (Plot 1 vs. Plot 2, $p=0.001$; vs. Plot 3, $p=0.0004$, vs. Plot 4, $p=0.0008$; vs. Plot 5, $p=0.0007$; vs. Plot 6, $p=0.0014$). All other plots were not significantly different from each other in respect to total P content as measured by ICP-AES by Tukey's comparison (for all, $p>0.05$), and were found to be non-significant by one-way ANOVA when data for Plot 1 were removed from the model ($F_{4,10}=0.6514$, $p=0.6389$). Removal of Plot 1 from the data set as identified by ROUT test gave a mean total P of 13.8 mg P. kg^{-1} across plots 2–6.

3.2 | Analysis of NaOH-EDTA extracts of soil by LC-ICP-MS

Soil extracts at soil mass:extractant ratio of 1 g:10 mL (Cade-Menun & Preston, 1996) were subjected to LC-ICP-MS without freeze-drying/reconstitution (concentration) required of NMR. HCl eluted D-*chiro*-, *myo*-, *neo*- and *scyllo*-inositol hexakisphosphates within 25 min (Figure 2). Excepting *myo*-$InsP_6$, the standards used were from the original collections of Max Tate and Dennis Cosgrove. The same standards, analysed as 10 pmol injections, yielded single predominant sharp peaks resolved from inorganic phosphate at 5.1 min (Figure S2).

LC-ICP-MS traces from sample 4A (a fertilized sample, from plot 4, subplot A) and the same spiked individually with ~100 µM (~1 nmol) D-*chiro*-, *myo*-, *neo*- and *scyllo*-inositol hexakisphosphate ($InsP_6$) are shown (Figure 2). Predominant peaks of inorganic phosphate, *myo*- and *scyllo*-$InsP_6$ are evident in sample 4A (Figure 2e). Each of the standards added a single predominant peak of inositol phosphate, a contribution to the inorganic phosphate peak and, for D-*chiro*-$InsP_6$, a minor peak representing a 'lower' *chiro*-inositol phosphate species at ca. 13.5 min (Figure 2a). For comparison, Smernik and Dougherty (2007) spiked 3.8 mL of NMR sample with ~29 nmol of sodium phytate, while Reusser, Verel, Frossard, et al. (2020) spiked ~600 µL NMR samples with 55 or 100 nmol to give signal ~3× that of un-spiked sample.

3.3 | Comparison of LC-ICP-MS and 31P NMR

To compare LC-ICP-MS and NMR, we conducted 31P NMR on a ground and sieved aliquot of sample 4C (a fertilized sample from plot 4, subplot C). Here, 0.5 g was extracted in 5 mL of NaOH-EDTA. From this, 500 µL was mixed with 25 µL of 30 mM methylenediphosphonic acid, 34 µL of NaOD and transferred to a 5-mm NMR tube. The sample, representing the NaOH-EDTA extract of 50 mg of soil, was subjected to NMR. The raw data, which are not fitted or deconvoluted, other than application of Fourier transform, phase and baseline correction, are shown (Figure 3a). Resonances typical of inositol phosphates were barely detectable. Following NMR, an aliquot (105 µL) was removed and its volume replaced with 50 µL

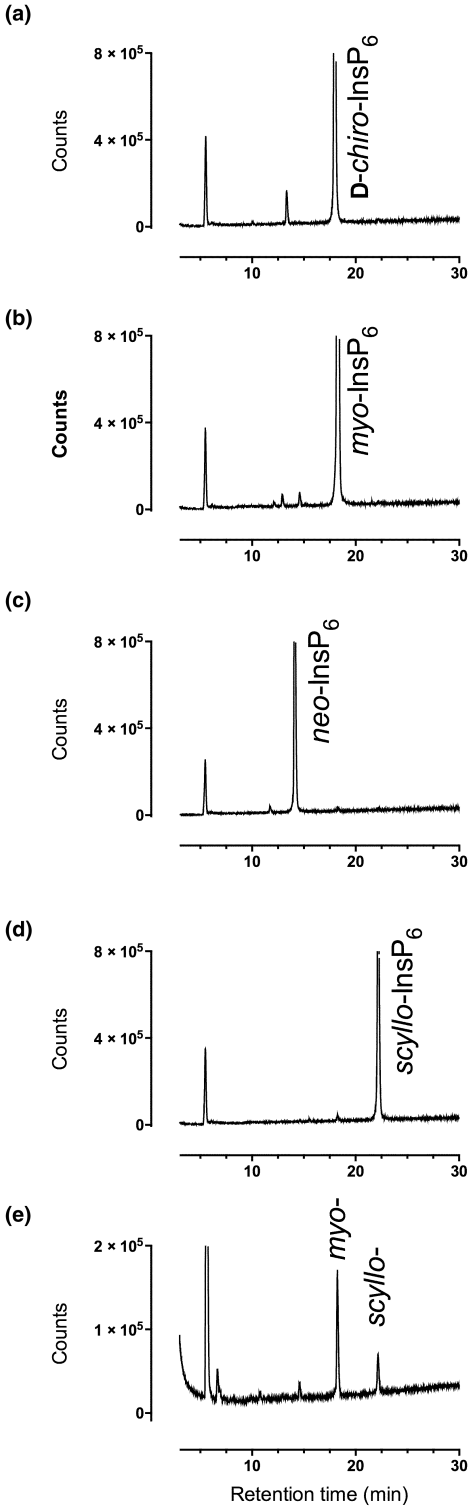

FIGURE 2 LC-ICP-MS of a soil extract spiked with different inositol hexakisphosphate standards. (a) Sample 4A spiked with D-*chiro*-$InsP_6$; (b) sample 4A spiked with *myo*-$InsP_6$; (c) sample 4A spiked with *neo*-$InsP_6$; (d) sample 4A spiked with *scyllo*-$InsP_6$; (e) Sample 4A. For all panels, 10 µL was injected.

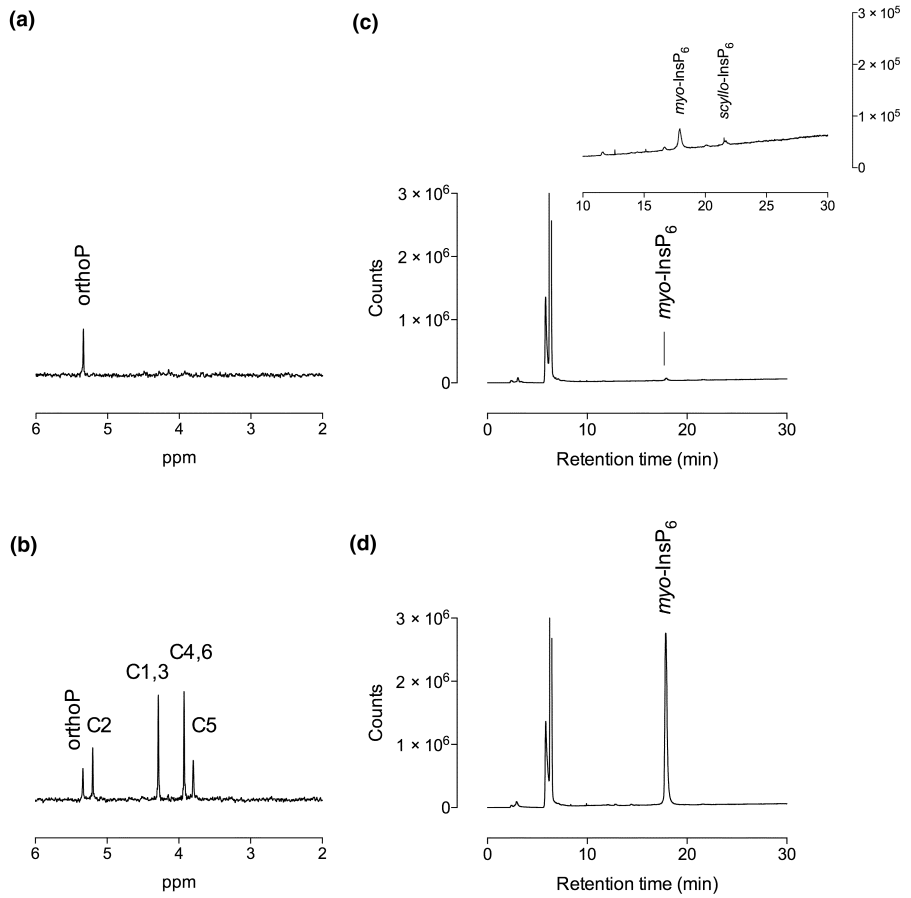

FIGURE 3 Comparison of methods of measurement of inositol phosphates in a soil extract. (a) 31P NMR of an NaOH-EDTA extract of soil (50 mg equivalent in 560 μL final volume). (b) 31P NMR of A after the removal of 100 μL, restoration to volume and spike with 1 μL 100 mM *myo*-$InsP_6$. The resonances of individual P nuclei in *myo*-$InsP_6$ are identified by locant (C2, C1/3, C4/6 and C5), that of orthophosphate is indicated (orthoP). (c) LC-ICP-MS analysis of PO^+ at m/z 47 of 10 μL of the sample analysed in (a); (d) LC-ICP-MS analysis of 13 μL of the sample analysed in (b). The inset in (c) is a 10-fold expansion of the *y*-scale.

18.2 Mohm cm water, 50 μL NaOH-EDTA, 4 μL 30% NaOD and 1 μL 100 mM *myo*-$InsP_6$. This spiked sample was subjected to NMR (Figure 3b) before removal of another aliquot. Small aliquots, 10 and 13 μL, respectively, of the two NMR samples were analysed by LC-ICP-MS (Figure 3c,d). The ~180 μM spike of *myo*-$InsP_6$ dominated the chromatogram of the spiked extract (Figure 3d). The integrated area of the *myo*-$InsP_6$ peak in Figure 3d was ~60× that of the *myo*-$InsP_6$ peak in the un-spiked sample (Figure 3c), which, nevertheless, also showed discernible peaks of *scyllo*-$InsP_6$ and 'lower' inositol phosphates (inset to Figure 3c).

For the spiked sample (Figure 3b), the sharp C2, C1/3, C4/6 and C5 resonances at 5.21, 4.29, 3.93 and 3.80 ppm have a summed, integrated intensity ~10× that of the orthophosphate resonance at 5.34, most of that signal arising from the soil extract. Additionally, the extract which was mildly diluted by the addition of NMR reagents before analysis in Figure 3a was separately diluted 10-fold with NaOH-EDTA and an aliquot of 100 μL was injected (Figure S3). The chromatograms generated from injections shown in Figure S3 and Figure 3c are more or less equivalent, both representing an extract of ~1 mg of soil on-column. These data highlight the difference in sensitivity of LC-ICP-MS and 31P NMR.

To assess the robustness of LC-ICP-MS with larger samples, three separate extractions of 0.5 g of a ground and sieved soil sample are shown (Figure 4). The coefficients of variation of peak area, a product of run-to-run instrument variability and extraction reproducibility, for *myo*-$InsP_6$ and *scyllo*-$InsP_6$ were 0.055 and 0.049, respectively.

With confidence in the sensitivity and reproducibility of LC-ICP-MS, the soil samples of Figure 1 were subjected to LC-ICP-MS. We chose not to homogenize samples because we sought to elaborate the possibility of local (mm scale) variation in soil inositol phosphates. As example, the six samples of Figure 5 show striking variability in soil inositol phosphate content, predominant peaks of *myo*- and *scyllo*-$InsP_6$ in all samples and multiple peaks of less abundant isomers.

3.4 | Analysis of speciation of 'lower' inositol phosphates in soil by LC-ICP-MS

Spiking of samples with authentic standards is essential for identification of inositol phosphates by peak position (chemical shift) in NMR

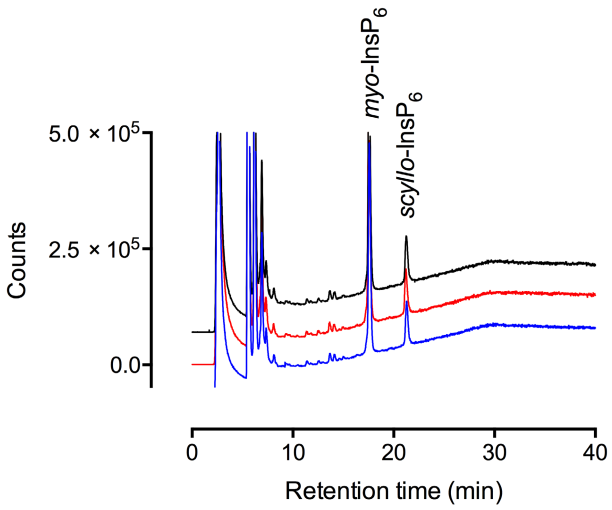

FIGURE 4 Reproducibility of LC-ICP-MS of NaOH-EDTA extracts. Aliquots (100 μL) of three separate extractions in 1:10 mass: volume ratio of a ground and sieved sample are shown in blue, red and black, with traces offset on the *y*-axis for clarity.

experiments. Figure 6 compares the elution of a soil sample (Figure 6a) and a set of standards obtained by acid hydrolysis of *myo*-$InsP_6$ (Figure 6b). Peaks with identical retention times to inositol phosphates previously identified in *myo*-$InsP_6$ hydrolysates (Blaabjerg et al., 2010; Chen & Li, 2003; Whitfield et al., 2018, 2020) are numbered 1–10 and peaks in the soil sample that are not clearly represented in the hydrolysate are identified a–e, with e identified as *scyllo*-$InsP_6$ (see Figure 2, Figure S2). Notwithstanding the ability of chromatography (Figure 2, Figure S2) to separate all known inositol hexakisphosphates yet identified in soil nor the consistency of LC (retention time) and ICP-MS detector response (Figure 4), a separate sample of soil 4C, was spiked with D-*chiro*-$InsP_6$, *neo*-$InsP_6$ and *scyllo*-$InsP_5$ before chromatography. The chromatograms from the original and spiked sample are shown in Figure 7a and that of the diluted (with *myo*-$InsP_6$ hydrolysate) sample is similarly overlaid with the original in Figure 7b. Precise co-elution of soil peaks with standards is revealed. The co-elution of peak d (Figure 6a) with *scyllo*-$InsP_5$ (*scyllo*-Ins(1,2,3,4,5)P_5) (Figure 7a) identifies 'd' as *scyllo*-$InsP_5$, wholly separable from all *myo*-$InsP_5$s (Whitfield et al., 2018, 2020). The *neo*-$InsP_6$ standard co-eluted precisely with

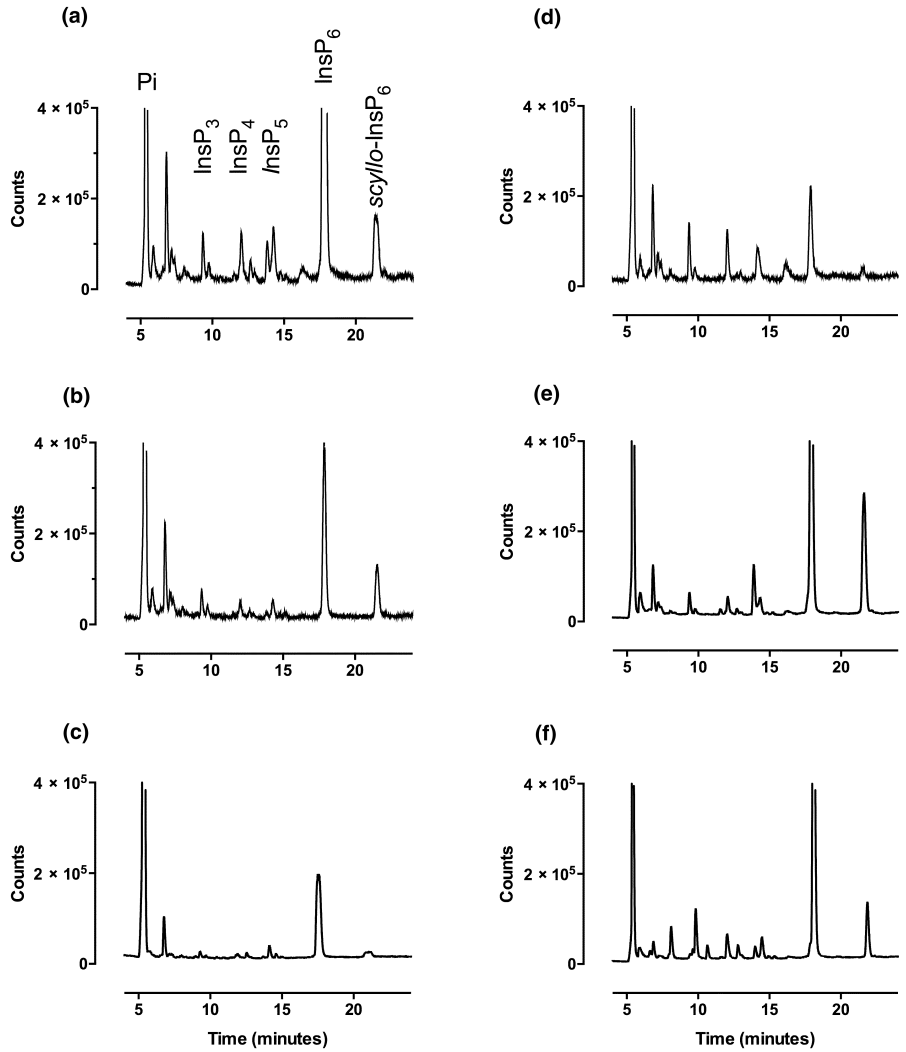

FIGURE 5 Example of LC-ICP-MS analysis of inositol phosphates extracted from soils. (a–c) Control plots 1–3A; (d–f), N-fertilized plots 4–6A. For brevity, labels, Pi, inorganic phosphate; and different inositol phosphates, *myo*-$InsP_3$–$InsP_6$ and *scyllo*-$InsP_6$, are added only to panel (a). 100-μL injection.

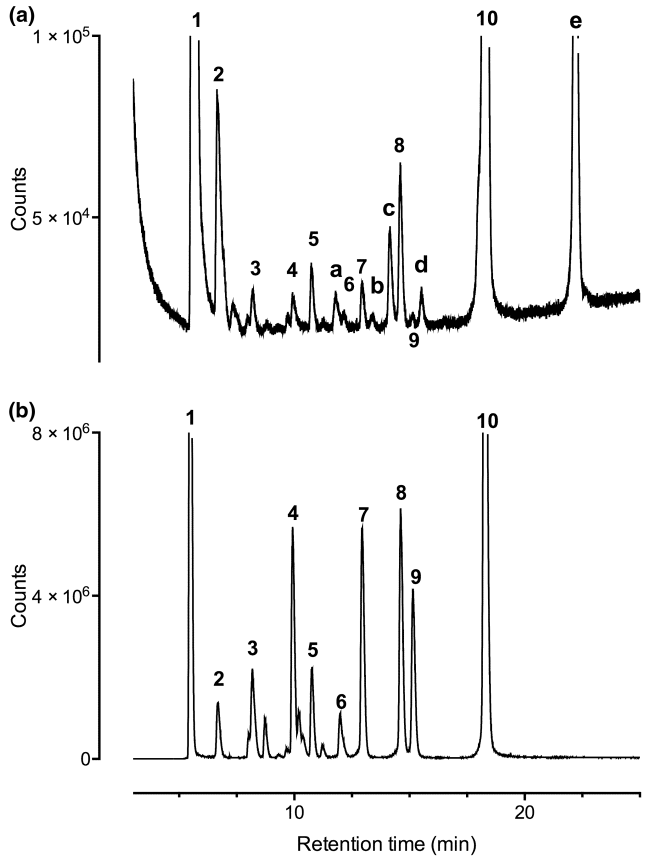

FIGURE 6 Speciation of inositol phosphates in soil samples. (A) Sample 1A; (B) an acid hydrolysate of *myo*-InsP_6. The peaks identified are 1, inorganic phosphate; 2, *myo*-InsP_2 isomer(s) unknown; 3, *myo*-InsP_3 isomer(s) unknown; 4, D/L-*myo*-Ins(1,2,3,4)P_4 and/or *myo*-Ins(1,3,4,6)P_4; 5, D/L-*myo*-Ins(1,2,5,6)P_4; 6, D/L-*myo*-Ins(1,4,5,6)P_4; 7, D/L-*myo*-Ins(1,2,3,5,6)P_5; 8, D/L-*myo*-Ins(1,2,4,5,6)P_5; 9, *myo*-Ins(1,3,4,5,6)P_5; 10, *myo*-InsP_6; a, unknown isomer; b, unknown isomer; c, unknown isomer; d, unknown isomer; e, *scyllo*-InsP_6.

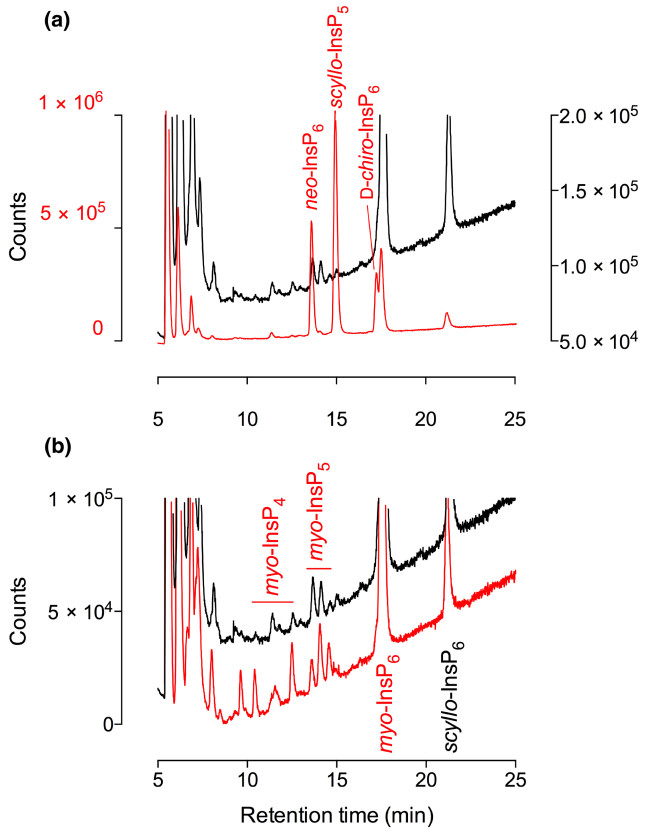

FIGURE 7 Speciation of inositol phosphates in soil samples: spiking experiments. (a), sample 4C (black trace) and the same spiked with D-*chiro*-InsP_6, *neo*-InsP_6 and *scyllo*-InsP_5 (red trace). Traces displayed on separate *y*-scales: left, red; right, black. The elution positions of standards are labelled in red. (b) Sample 4C (data of A, on a different scale, black trace) and the same diluted with an acid-hydrolysate of *myo*-InsP_6 (red trace). *Myo*-inositol phosphate classes contained in the hydrolysate are labelled in red. Traces are shifted on the *y*-scale to aid inspection.

one that elutes among *myo*-inositol tetrakisphosphates (InsP_4s) (cf. Figure 7a,b), while the D-*chiro*-InsP_6 standard was resolved from the peak of *myo*-InsP_6 (Figure 7a). The early elution of *neo*-InsP_6 (Figures 2 and 7a, Figure S2) and the increase of retention time through the series InsP_2–InsP_6 for *myo*-inositol phosphates (Figure 6), together with previous descriptions of elution of *neo*-InsP_4, *neo*-InsP_5 and *neo*-InsP_6 (Whitfield et al., 2018), reveal that 'lower than hexakisphosphate' esters of *neo*-inositol elute considerably earlier than *myo*-InsP_4s. Although less certain, peaks a, b and c (Figure 6a) could include *scyllo*-InsP_4s. Among the peaks eluted, were those with the chromatographic behaviour of D/L-*myo*-Ins(1,2,3,4,5)P_5 and D/L-*myo*-Ins(1,2,4,5,6)P_5. The low abundance of InsP_5s relative to InsP_6 isomers is consistent with the observations of Irving and Cosgrove (1982) with other soils.

The column/acid eluent combination also has considerable resolving power for *myo*-InsP_4 species (Blaabjerg et al., 2010; Chen & Li, 2003; Whitfield et al., 2018, 2020). We detected peaks with the precise chromatographic mobility of D/L-*myo*-Ins(1,2,3,4)P_4 and/or *myo*-Ins(1,3,4,6)P_4, D/L-*myo*-Ins(1,2,5,6)P_4 and D/L-*myo*-Ins(1,4,5,6)P_4 (Figures 6 and 7), separable from ADP and ATP that elute earlier than *myo*-InsP_3 (Whitfield et al., 2020) and from pyrophosphate and metatriphosphate (Figure S4).

3.5 | Lack of effect of N-fertilization on soil inositol phosphate profile

With identities assigned to various peaks of inositol phosphate in Åsele forest soil, a comparison was made of fertilized and unfertilized plots, example traces of which are shown in Figure 5. The results of analysis of extractions of 18 soil samples 1A–C to 6A–C are shown in Table 2 with peaks assigned broadly to class by elution position, which is an excellent proxy for extent of phosphorylation. As described above, such a simplification risks misidentification of some of the minor components but, nevertheless, allows test of the effect of fertilization. The predominant inositol phosphate species identified were *myo*-InsP_6 and *scyllo*-InsP_6 (Table 2).

TABLE 2 Inositol phosphates in non-fertilized and N-fertilized soils. Non-fertilized soils 1–3 and N-fertilized soils 4–6 were analysed by LC-ICP-MS. Values given in mg P kg^{-1} fresh soil.

mg P kg^{-1}									
		[1]*myo-*					[1]*scyllo-*	∑[*myo-*, *scyllo*]	
[2]Soil	[3]Pi	[4]Pi + unknowns	$InsP_3$	$InsP_4$	$InsP_5$	$InsP_6$	$InsP_6$	∑[$InsP_3$-$InsP_6$]	[5]$tP_{NaOH\text{-}EDTA}$
1	19.44 ± 7.0[a]	32.62 ± 10.47[a]	0.1 ± 0.1[a]	0.1 ± 0.1	0.21 ± 0.1	7.13 ± 3.6[a]	1 ± 0.4	8.42 ± 4.1[a]	53.3 ± 16.9[a]
2	5.74 ± 2.4[b]	7.46 ± 2.740[b]	32.62 ± 10.47[a]	nd	0.06 ± 0.1	2.57 ± 2.9[a,b]	0.76 ± 0.7	3.39 ± 3.6[a,b]	14.9 ± 7.9[b]
3	3.74 ± 2.0[b]	5.06 ± 2.03[b]	32.62 ± 10.47[a]	0.01 ± 0.1	0.01 ± 0.02	0.99 ± 1.0[b]	0.28 ± 0.2	1.29 ± 1.2[b]	10.2 ± 2.7[b]
4	6.49 ± 4.2[b]	7.85 ± 4.35[b]	32.62 ± 10.47[a]	0.004 ± 0.1	0.03 ± 0.03	1.3 ± 0.7[a,b]	0.31 ± 0.2	1.64 ± 0.9[a,b]	13.9 ± 2.9[b]
5	6.53 ± 1.6[b]	7.75 ± 1.71[b]	0.01 ± 0.02[b]	0.02 ± 0.03	0.07 ± 0.1	1.33 ± 1.3[a,b]	0.47 ± 0.4	1.9 ± 1.8[a,b]	13.4 ± 5.3[b]
6	8.35 ± 3.4[b]	9.65 ± 3.33[b]	nd[b]	0.01 ± 0.02	0.06 ± 0.07	2.04 ± 1.7[a,b]	0.42 ± 0.3	2.52 ± 2.0[a,b]	16.3 ± 3.3[b]
ANOVA									
p-value	0.0044	0.0002	0.0031	0.8415	0.1406	0.0353	0.2034	0.0415	0.0003

Note: Significant differences of individual or aggregated species between plots are indicated by the absence of common superscript letter (Tukey, $p < 0.05$).

Abbreviation: nd, not detected.

[1]Inositol phosphates measured by LC-ICP-MS are aggregated into individual classes: $InsP_3$, $InsP_4$, etc.

[2]Soils represented as means of subplot measurements (A-C) ± Standard Deviation. 1–3, non-fertilized; 4–6, fertilized.

[3]The 'Pi' peak coelutes with $InsP_1$ and likely includes other unknown organic phosphates.

[4]The 'Pi' peak is summed with unknown compounds eluting before $InsP_3$.

[5]$tP_{NaOH\text{-}EDTA}$, total phosphorus measured by ICP-AES (data of Figure 1).

Analysis by one-way ANOVA showed that total NaOH-EDTA-extractable P varied among the plots (Figure 1, $p = 0.0003$). Similarly, individual and total inositol phosphates also varied significantly between plots (Table 2), but only because of the departure of Plot 1 from all other plots. When plots were pooled within each treatment to give nine replicates and tested by a two-tailed Student's *t*-test with Welch's correction, there was no significant difference in total inositol phosphates with long-term N-fertilization (∑*myo*-[$InsP_3$-$InsP_6$], *scyllo*-$InsP_6$ $p = 0.1462$). Thus, while significant difference was noted by ANOVA between non-fertilized soils 1 and 3 in respect of Pi, $InsP_3$, *myo*-$InsP_6$ and $tP_{NaOH\text{-}EDTA}$—this difference did not extend to other classes of inositol phosphates or to the aggregated total of inositol phosphates.

Phosphorus recovered as the sum of inositol phosphates, inorganic phosphate and unidentified peaks (eluting at 5–7.9 min) accounted for 77.1%, 72.9%, 62.0%, 68.2%, 71.8% and 74.5%, respectively, of $tP_{NaOH\text{-}EDTA}$ of Plots 1–6 (Table 2). The early eluting peaks (Figure 5) include inorganic phosphate and could include 'humic' substances. We anticipate further development of LC-ICP-MS will include tandem UV detection to identify UV-absorbing components in soil extracts. A recent study employing sequential chemical fractionation (Reusser et al., 2023) indicates that, in the soils studied, recovery of inositol phosphates was not complete in NaOH-EDTA. The LC-ICP-MS method offers opportunity to probe the distribution of inositol phosphate species between different fractions obtained by SCF.

Further analysis of Table 2, to compare the ratio *myo*-$InsP_6$: *scyllo*-$InsP_6$, is shown in Figure 8. Whether data were pooled or not, there was no difference in ratio between treatments, that is despite marked difference in total NaOH-EDTA-extractable P (10.2–53.3 mg kg^{-1}, as plot means, Table 2), or 6.8–66.9 mg P. kg^{-1} as individual subplots (Figure 1). The ratios of *myo*-$InsP_6$: *scyllo*-$InsP_6$ were not different between control and N-fertilized plots (Welch's *t*-test for pooled treatment means, $p = 0.8708$).

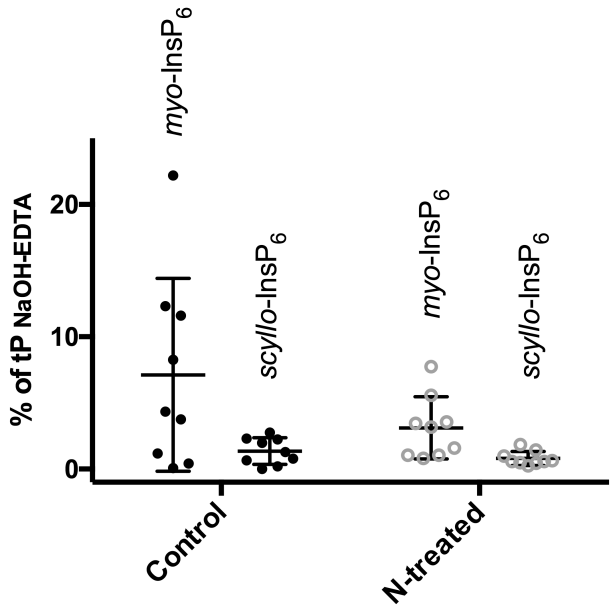

FIGURE 8 Independence of *myo*-$InsP_6$ and *scyllo*-$InsP_6$ content of soil on N-fertilization status. Mean and standard deviation ($n = 9$) of *myo*- and *scyllo*-$InsP_6$ fractions expressed as % of NaOH-EDTA-extractable P.

3.6 | Accessing variation in soil organic phosphate distribution on mm scale

To explore the limits of sampling, we took nine individual 10-mg samples from soil 4C (plot 4, subplot C) and extracted each with 0.1 mL of NaOH-EDTA. In parallel, we took 2 g of the same sample and ground it to pass through a 1.4-mm sieve before taking nine individual 10-mg portions for extraction in the same volume. The LC traces of two of each of the dispersed samples and homogenized (ground) portions that represent the extreme outliers of detector response for each set are shown (Figure 9).

Microsampling identified peaks similar to those detected from the larger (NMR-scale) regimen (cf. Figures 2–4). Both *myo*-$InsP_6$ and *scyllo*-$InsP_6$ were identified (Figure 9). For the non-ground and non-sieved soil shown (Figure 9a,b), the variability represents a product of run-to-run instrument variability and reproducibility of extraction, which is low for 0.5 g samples, Figure 4, and its interaction with natural spatial variation (non-uniformity of distribution) of organic material within sample 4C. The coefficients of variation for *myo*-$InsP_6$ and *scyllo*-$InsP_6$ contents were 1.589 and 1.141, respectively. For the ground/sieved portions (Figure 9c,d), the natural spatial variation has been removed by homogenization. Consequently, the coefficients of variation for *myo*-$InsP_6$ and *scyllo*-$InsP_6$ are smaller, 0.143 and 0.256, respectively. Here, the coefficients represent the product of run-to-run instrument variability and reproducibility of extraction of otherwise identical samples. These coefficients can be directly compared with those (0.055, *myo*-$InsP_6$ and 0.049, *scyllo*-$InsP_6$) from the larger scale (0.5 g) extraction of a ground/sieved soil (Figure 4). These comparisons define the boundaries of LC-ICP-MS for analysis of the soils studied here. Separately, they reveal non-uniformity of inositol phosphate content of soil on 10-mg scale or mm scale, and the suitability of LC-ICP-MS for investigation of this.

Figure 10 shows the inositol phosphate speciation of these non-sieved (NS) or sieved (S) samples, expressed per kg of soil. That the means of the individual inositol phosphates are numerically similar, is coincidental. There are 200 individual 10-mg samples in 2 g of the NS sample and we sampled nine of these. We have no reason to assume that, within the nine, we have found the outliers or the 'best' representatives of these. Here, the underlying extraction and run-to-run instrument variability of the 'measurement' of NS is represented by the error (sd) bars of S, the natural non-uniformity of the samples increases the error bars. The proportions of the different classes of inositol phosphates identified were approximately 1.3%, 2.5%, 7.6%, 73.3% and 15.1%, respectively, for *myo*-$InsP_3$, *myo*-$InsP_4$, *myo*-$InsP_5$, *myo*-$InsP_6$ and *scyllo*-$InsP_6$.

To put local non-uniformity of organic P in context of inputs to soil, three extractions of single seeds of Arabidopsis are shown

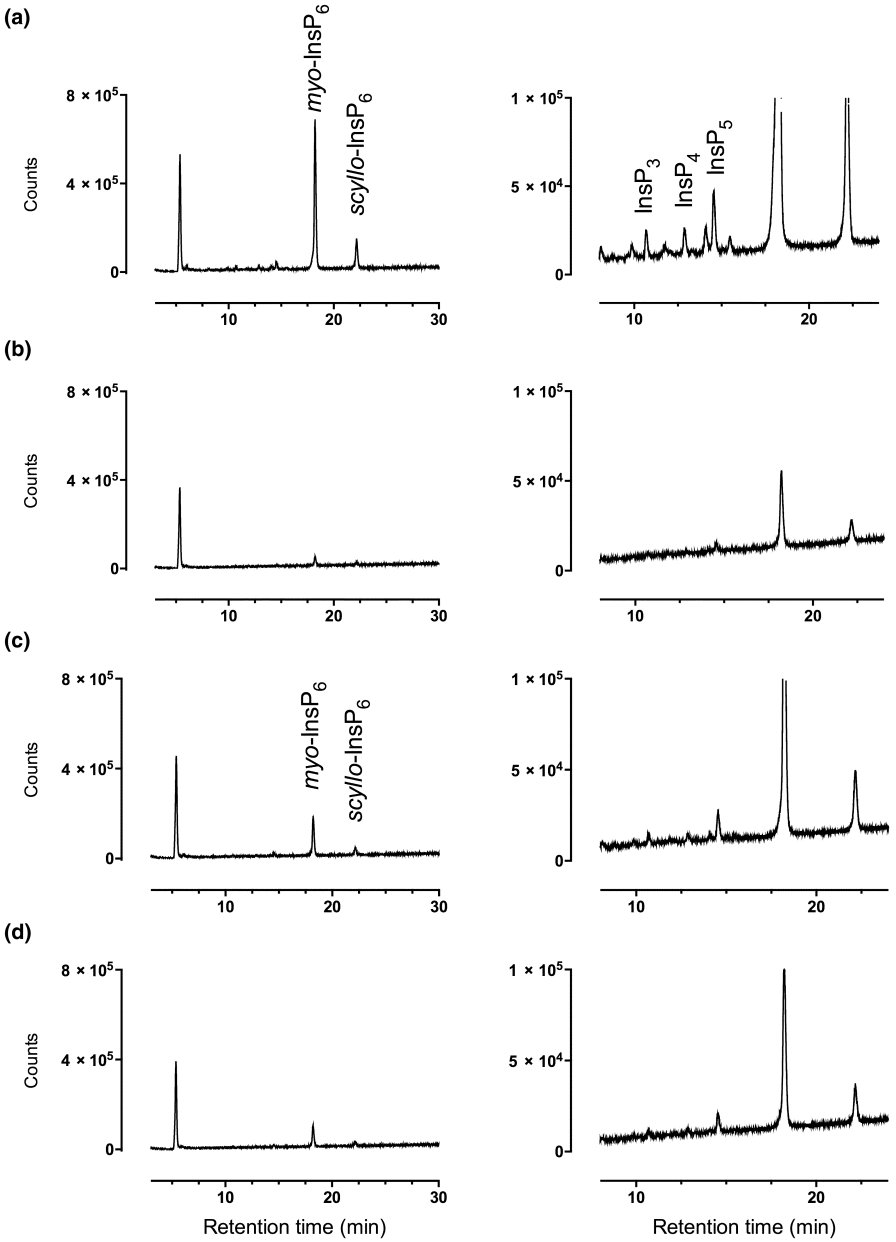

FIGURE 9 LC-ICP-MS separation and detection of inositol phosphates in hydroxide-EDTA extracts of 10-mg soil samples. Individual samples representing the outliers of detector response for nine individual samples of non-sieved soil 4C (a, b) or portions of sieved soil 4C (c, d) were analysed by LC-ICP-MS at m/z 47. The panels on the right are expansions of those on the left. Classes of inositol phosphates common to all samples are labelled in (a and c). 10-μL injections.

(Figure S5). The Col0 accession used has an average seed size (cross sectional area = 120,000 μm^2) and mass of ca. 28 μg (Herridge et al., 2011). Predominant peaks of inorganic phosphate and *myo*-$InsP_6$ were detected, representing approximately 30% and 70% of total P, respectively. Minor peaks of D- and/or L-*myo*-Ins(1,2,3,4,5)P_5 and D- and/or L-*myo*-Ins(1,2,4,5,6)P_5, representing less than 2% of total P were clearly detected (peaks b and c) and with data smoothing putative peaks of other *myo*-inositol pentakisphosphates (peaks a and d) could be discerned, but neither D-*chiro*-, *neo*- nor *scyllo*-inositol hexakisphosphate was detected.

4 | DISCUSSION

Considerable variation in organic P and phytate is reported in different soils (Smernik & Dougherty, 2007; Turner et al., 2002). Variation may have arisen through the use of disparate methodologies, through mis-identification of phytate resonances in 31P NMR (Smernik & Dougherty, 2007) or because of spatial variation. Partly for these reasons, we have sought to develop a methodology that is compatible with the NaOH-EDTA extraction regimen that has been the foundation of 31P NMR analyses of many groups and which, by chromatography, separates inositol phosphates from the 'humic' fraction.

Setting aside the general absence in the literature, as here, of study of the same soil by different groups, for the Åsele soil, total P (tP) of N-fertilized and unfertilized plots bound the values of ca. 18–22 mmol/kg (558–682 mg kg^{-1}) reported for the organic layer of Swedish, Tärnsjö and Tönnersjöheden, forest soils (Figure 1, Adediran et al., 2020). Of these, organic P represented the major P fraction at ~17–19 mmol kg^{-1} (Figure 1, Adediran et al., 2020). Median values of 0.50–0.180 mg kg^{-1} of organic P were measured for the 0–10 cm mineral soil layer of Scandinavian soil (Spohn & Stendahl, 2022), with total P (assumed all

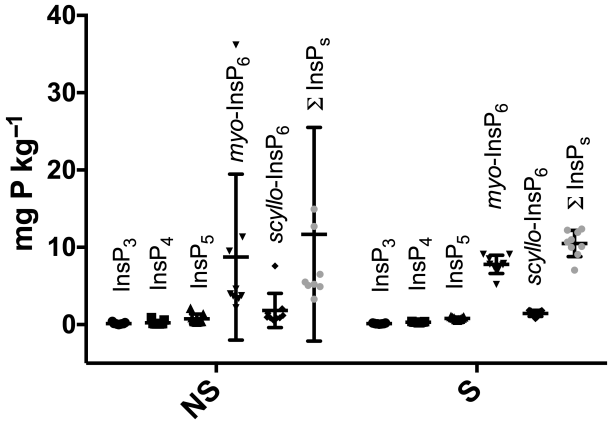

FIGURE 10 Speciation of inositol phosphates in hydroxide-EDTA extracts of 10-mg soil samples. Nine individual samples of a soil (NS) were analysed by LC-ICP-MS at m/z 47. Separately, the soil was homogenized by grinding and sieving (S) and nine portions of this processed soil were analysed. Mean and standard deviation are shown.

to be organic) of the parental material (organic layer) in most of more than 300 soils less than 1 mg kg^{-1}.

The data shown here confirm the resolving power of LC-ICP-MS for different inositol hexakisphosphates found in soil and for $InsP_4$ and $InsP_5$ species. One caveat is that the early (among inositol hexakisphosphates) elution of *neo*-$InsP_6$ places *neo*-$InsP_6$ in part of the chromatogram where *myo*-$InsP_4$s elute, albeit as minor fractions. Equally uncertain, early eluting peaks could include *scyllo*-$InsP_4$s, of which there are three possible isomers (Thomas et al., 2016), or *chiro*-$InsP_5$s. In some samples, the *myo*-$InsP_6$ peak had a very minor (earlier-eluting) shoulder that could be *chiro*-$InsP_6$. Again, as for other soils (Reusser, Verel, Frossard, et al., 2020), this is a minor component. The existence of lower esters of *chiro*, *myo*-, *neo*- and *scyllo*-inositol phosphates, albeit as minor components, was reported in seminal studies (Anderson, 1955; Cosgrove, 1963; Halstead & Anderson, 1970; McKercher & Anderson, 1968a, 1968b) and more recently (Reusser, Verel, Zindel, et al., 2020). The latter identified D- and/or L-*myo*-Ins(1,2,4,5,6)P_5 and *myo*-Ins(1,3,4,5,6)P_5, *scyllo*-$InsP_5$ and unspecified *neo*- and *chiro*-$InsP_5$ species.

Perhaps, more noteworthy is the gain in sensitivity obtained by LC-ICP-MS, one–two orders of magnitude more sensitive than UV detection of ferric complexes (Whitfield et al., 2020). LC-ICP-MS can measure less than a single pmol on column. To put this in context of ^{31}P NMR, which typically uses ~25%–50% of the sample extracted from 1 g equivalent of soil (Cade-Menun & Preston, 1996; Doolette et al., 2011), LC-ICP-MS measures multiple inositol phosphates in samples of 10 mg and can measure *myo*- and *scyllo*-$InsP_6$ in extracts equivalent of a single mg of soil.

An added advantage is that detector response is directly proportional to P content, independent of degree of phosphorylation of separated species. The relative size of the peaks accurately reflects the amount of P in each species. Unlike for ^{31}P NMR, in which total signal for an individual inositol phosphate species is divided among the discrete resonances of individual P nuclei (the nuclei of the phosphate substituents on the inositol ring that are given individual locants, 1-, 2-. 3-, 4-, 5- and -6), in LC-ICP-MS a single peak gives the total P signal for an individual inositol phosphate. Even so, distinct inositol phosphate species can co-elute in LC. Conveniently, LC-ICP-MS has a cycle time of 50 min, that could be shortened, contrasting with the 1–2 days required of 31P NMR when recycle delays of up to 30 s, to allow full T1 relaxation, and 1024 or 4096 scans are demanded (Reusser, Verel, Zindel, et al., 2020).

While there has been little systematic research on the inositol phosphate profile of plant tissues other than storage organs (Raboy, 2003), *myo*-inositol hexakisphosphate is considered a major input to soil organic phosphate (Turner et al., 2002). Here, the ability of LC-ICP-MS and ^{31}P NMR (Reusser, Verel, Zindel, et al., 2020) to identify isomers bearing, or not, a 2-phosphate, is descriptive of the origin of these isomers: Those with a 2-phosphate are most likely products of phytate turnover, those without are synthetic precursors (Irvine & Schell, 2001). The isomers measured by LC-ICP-MS in a single Arabidopsis seed is typical of bulk measurement of Arabidopsis (Bentsink et al., 2003), of seeds in general (Raboy, 2003) and highlights the use of LC-ICP-MS for analysis of local accretions of organic material.

While N inputs are reported to increase P limitation of ecosystems (Cunha et al., 2022) and increase soil enzymes associated with P cycling (Margalef et al., 2021; Papanikolaou et al., 2010), other studies report no effect on soil enzyme activities (Turner & Wright, 2014). We note that degradation of different phytates, D-*chiro*-, *myo*-, *neo*- and *scyllo*-, is not described in situ in soil at the level of speciation of 'lower' inositol phosphates. Consequently, the data do not allow comment on the enzymology of phytate turnover in control and N-fertilized plots. Nevertheless, there was no differential effect of fertilization on a specific isomer.

LC-ICP-MS offers analyses formerly only accessible to 31P NMR. It is quicker, less intensive in sample workup and more sensitive. It offers opportunity for two- and three-dimensional mapping of hydroxide-extractable organic and inorganic P in soil. Here, our analysis of Åsele soil can be placed in context of Scandinavian soils, for which landscape-scale surveys of soil P are reported (Ballabio et al., 2019; Spohn & Stendahl, 2022) and for which organic P content was shown to increase as particle size decreases (Spohn, 2020; Spohn & Stendahl, 2022). By microsampling, LC-ICP-MS allows the speciation of organic P on scales approaching single mm resolution. Microscale resolution of P-binding to soil mineral particles has been described (Adediran et al., 2020, 2022). Separately, LC-ICP-MS could be an ideal tool to study the P dynamics of experimental microcosms, such as mycorrhizal split-root systems containing fungal and microbial partners (Schreider et al., 2022).

5 | CONCLUSIONS

As plant material is a major input to soil, with seeds especially enriched with *myo*-inositol hexakisphosphate, demonstration of how

point foci of inositol phosphate abundance within soil samples can be studied by LC-ICP-MS offers opportunity for the study of the origin(s) of *chiro*-, *neo*- and *scyllo*-isomers of inositol phosphates in soil.

The method bridges gaps of physical scale and chemical speciation between pore-scale analysis of organic versus inorganic P-speciation by techniques such as K-edge X-ray absorption near-edge structure spectroscopy and X-ray fluorescence microscopy and more common aggregated sample analyses of soil P by ^{31}P NMR.

We anticipate the mapping of inositol phosphates in the rhizosphere and soil particle size-fractionated measurements of inositol phosphates. Particle size is an important discriminator of organic phosphate content of boreal soils that relates to environmental and pedogenic parameters such soil age, mean annual precipitation and mean annual temperature.

It is striking that long-term soil N-fertilization had no significant impact on inositol phosphate concentrations, whether expressed in absolute terms or relative to the total P in the soil. Increasing N availability frequently results in increased activity of P-degrading enzymes and changes a suite of other properties that likely impact rates of biogeochemical cycling. Further work is needed to better understand the turnover of inositol phosphates; the method described here is ideally suited to this endeavour.

AUTHOR CONTRIBUTIONS

Charles A. Brearley, Colleen Sprigg and Graham Chilvers conceived novel analytical methodology and implemented it. Megan Barker, Filipa Cox and David Johnson conceived and executed forest experiments, collected and analysed data therefrom. Joseph Carroll and Ignacio Delso performed analytical experiments, collected data and analysed data. Charles A. Brearley, David Johnson and Colleen Sprigg led the writing of the manuscript. All authors made critical contributions to the draft and gave final approval for publication. Our study accessed soils from forest managed by Skogforsk, Uppsala, Sweden. Underpinning work from staff of Skogforsk was cited.

ACKNOWLEDGEMENTS

This work was supported by a BBSRC Norwich Research Park Doctoral Training Studentship (Ref. BB/M011216/1) to CS and NERC (Ref. NE/W000350/1) grant to CAB. It was enabled by inositol phosphate samples originating from the collections of the late Dennis Cosgrove and the late Max Tate. We thank staff of Skogforsk, Uppsala, Sweden, for the management of the site from which soil samples were taken.

CONFLICT OF INTEREST STATEMENT

The authors declare that they have no conflicts of interest.

PEER REVIEW

The peer review history for this article is available at https://www.webofscience.com/api/gateway/wos/peer-review/10.1111/2041-210X.14292.

DATA AVAILABILITY STATEMENT

Data, *x*, *y* values from which chromatograms were plotted, including system peaks (Rugova et al., 2014) are archived at https://research-portal.uea.ac.uk/en/persons/charles-brearley/datasets/ (Carroll et al., 2023).

ORCID

Charles A. Brearley https://orcid.org/0000-0001-6179-9109

REFERENCES

Adediran, G. A., Kielman-Schmitt, M., Kooijmaan, E., & Gustafsson, J. P. (2022). Significance of phosphorus inclusions and discrete micron-sized grains of apatite in postglacial forest soils. *European Journal of Soil Science*, *73*, e13310. https://doi.org/10.1111/ejss.13310

Adediran, G. A., Tuyishime, J. R. M., Vantelon, D., Klysubun, W., Gustafsson, J. P., & Simonsson, M. (2020). Phosphorus in 2D: Spatially resolved P speciation in two Swedish forest soils as influenced by apatite weathering and podzolization. *Geoderma*, *376*, 114550. https://doi.org/10.1016/j.geoderma.2020.114550

Anderson, G. (1955). Paper chromatography of inositol phosphates. *Nature*, *175*, 863–864.

Ballabio, C., Lugato, E., Fernández-Ugalde, O., Orgiazzi, A., Jones, A., Borrelli, P., Montanarella, L., & Panagos, P. (2019). Mapping LUCAS topsoil chemical properties at European scale using Gaussian process regression. *Geoderma*, *355*, 113912. https://doi.org/10.1016/j.geoderma.2019.113912

Bardgett, R. D., van der Wal, R., Jónsdóttir, I. S., Quirk, H., & Dutton, S. (2007). Temporal variability in plant and soil nitrogen pools in a high-artic ecosystem. *Soil Biology and Biochemistry*, *39*(8), 2129–2137. https://doi.org/10.1016/j.soilbio.2007.03.016

Bentsink, L., Yuan, K., Korneef, M., & Vreugdehil, D. (2003). The genetics of phytate and phosphate accumulation in seeds and leaves of *Arabidopsis thaliana*, using natural variation. *Theoretical and Applied Genetics*, *106*(7), 1234–1243. https://doi.org/10.1007/s00122-002-1177-9

Blaabjerg, K., Hansen-Moller, J., & Poulsen, H. D. (2010). High-performance ion chromatography method for separation and quantification of inositol phosphates in diets and digesta. *Journal of Chromatography. B, Analytical Technologies in the Biomedical and Life Sciences*, *878*(3–4), 347–354. https://doi.org/10.1016/j.jchromb.2009.11.046

Cade-Menun, B. J., Liu, C. W., Nunlist, R., & McColl, J. G. (2002). Soil and litter phosphorus-31 nuclear magnetic resonance spectroscopy. *Journal of Environmental Quality*, *31*(2), 457–465. https://doi.org/10.2134/jeq2002.0457

Cade-Menun, B. J., & Preston, C. M. (1996). A comparison of soil extraction procedures for 31P NMR spectroscopy. *Soil Science*, *161*(11), 770–785. https://doi.org/10.1097/00010694-199611000-00006

Carroll, J. J., Sprigg, C., Chilvers, G., Delso, I., Barker, M., Cox, F., Johnson, D., & Brearley, C. A. (2023). Data From: LC-ICP-MS analysis of inositol phosphate isomers in soil offers improved sensitivity and fine-scale mapping of inositol phosphate distribution. Brearley, C. (Creator), Wiley, 27 Dec 2023.

Chen, J., van Groenigen, K. J., Hungate, B. A., Terrer, C., van Groenigen, J.-W., Maestre, F. T., Ying, S. C., Luo, Y., Jörgensen, U., Sinsabaugh, R. L., Oelesn, J. E., & Elsgaard, L. (2020). Long-term nitrogen loading alleviates phosphorus limitation in terrestrial ecosystems. *Global Change Biology*, *26*(9), 5077–5086. https://doi.org/10.1111/gcb.15218

Chen, Q.-C., & Li, B. W. (2003). Separation of phytic acid and other related inositol phosphates by high-performance ion chromatography and its applications. *Journal of Chromatography A*, *1018*(1), 41–52. https://doi.org/10.1016/j.chroma.2003.08

Cosgrove, D. J. (1963). The chemical nature of soil organic phosphorus. I. Inositol phosphates. *Australian Journal of Soil Research*, *1*, 203–214. https://doi.org/10.1071/SR9630203

Cunha, H. F. V., Andersen, K. M., Lugli, L. F., Santana, F. D., Aleixo, I. F., Moraes, A. M., Garcia, S., Di Ponzio, R., Mendoza, E. O., Brum, B., Rosa, J. S., Cordeiro, A. L., Portela, B. T. T., Ribeiro, G., Coelho, S. D., de Souza, S. T., Silva, L. S., Antonieto, F., Pires, M., … Quesada, C. A. (2022). Direct evidence for phosphorus limitation on Amazon forest productivity. *Nature*, *608*(7923), 558–562. https://doi.org/10.1038/s41586-022-05085-2

Doolette, A. L., & Smernik, R. J. (2015). Quantitative analysis of 31P NMR spectra of soil extracts-dealing with overlap of broad and sharp signals. *Magnetic Resonance in Chemistry*, *53*(9), 679–685. https://doi.org/10.1002/mrc.4212

Doolette, A. L., Smernik, R. J., & Dougherty, W. J. (2009). Spiking improved solution phosphorus-31 nuclear magnetic resonance identification of soil phosphorus compounds. *Soil Science Society of America Journal*, *73*(3), 919–927. https://doi.org/10.2136/sssaj2008.0192

Doolette, A. L., Smernik, R. J., & Dougherty, W. J. (2010). Rapid decomposition of phytate applied to a calcareous soil demonstrated by a solution 31P NMR study. *European Journal of Soil Science*, *61*(4), 563–575. https://doi.org/10.1111/j.1365-2389.2010.01259.x

Doolette, A. L., Smernik, R. J., & Dougherty, W. J. (2011). Overestimation of the importance of phytate in NaOH-EDTA soil extracts as assessed by 31P NMR analyses. *Organic Geochemistry*, *42*(8), 955–964. https://doi.org/10.1016/j.orggeochem.2011.04.004

Gerke, J. (2010). Humic (organic matter)-Al(Fe)-phosphate complexes: An underestimated phosphate form in soils and source of plant-available phosphate. *Soil Science*, *175*(9), 417–425. https://doi.org/10.1097/SS.0b013e3181f1b4dd

Giesler, R., Esberg, C., Lagerström, A., & Graae, B. J. (2012). Phosphorus availability and microbial respiration across different tundra vegetation types. *Biogeochemistry*, *108*(1), 429–445. https://doi.org/10.1007/s10533-011-9609-8

Giles, C. D., Cade-Menun, B. J., & Hill, J. E. (2011). The inositol phosphates in soils and manures: Abundance, cycling, and measurement. *Canadian Journal of Soil Science*, *91*, 397–416. https://doi.org/10.4141/cjss09090

Halstead, R. L., & Anderson, G. (1970). Chromatographic fractionation of organic phosphates from alkali, acid, and aqueous acetylaceton extracts of soils. *Canadian Journal of Soil Science*, *50*, 111–119. https://doi.org/10.4141/cjss70-018

Herridge, R. P., Day, R. C., Baldwin, S., & Macknight, R. C. (2011). Rapid analysis of seed size in Arabidopsis for mutant and QTL discovery. *Plant Methods*, *7*(1), 3. https://doi.org/10.1186/1746-4811-7-3

Irvine, R. F., & Schell, M. J. (2001). Back in the water: The return of the inositol phosphates. *Nature Reviews. Molecular Cell Biology*, *2*(5), 327–328. https://doi.org/10.1038/35073015

Irving, G. C., & Cosgrove, D. J. (1981). The use of hypobromite oxidation to evaluate two current methods for the estimation of inositol polyphosphates in alkaline extracts of soils. *Communications in Soil Science and Plant Analysis*, *12*(5), 495–509. https://doi.org/10.1080/00103628109367169

Irving, G. C. J., & Cosgrove, D. J. (1982). The use of gas liquid chromatography to determine the proportions of inositol isomers present as pentakis and hexakisphosphates in alkaline extracts of soils. *Communications in Soil Science and Plant Analysis*, *13*, 957–967. https://doi.org/10.1080/00103628209367324

Jacobson, S., & Pettersson, F. (2010). An assessment of different fertilization regimes in three boreal coniferous stands. *Silva Fennica*, *44*(5), 123. https://doi.org/10.14214/sf.123

Jarosch, K. A., Doolette, A. L., Smernik, R. J., Tamburini, F., Frossard, E., & Bünemann, E. K. (2015). Characterisation of soil organic phosphorus in NaOH-EDTA extracts: A comparison of 31P NMR spectroscopy and enzyme addition assays. *Soil Biology and Biochemistry*, *91*, 298–309. https://doi.org/10.1016/j.soilbio.2015.09.010

Johnson, D., Leake, R. J., & Lee, J. A. (1999). The effects of quantity and duration of simulated pollutant and nitrogen deposition on root-surface phosphatase activities in calcareous and acid grasslands: A bioassay approach. *New Phytologist*, *141*(3), 433–442. https://doi.org/10.1046/j.1469-8137.1999.00360.x

Johnson, D., Leake, R. J., & Read, D. J. (2005). Liming and nitrogen fertilization affects phosphatase activities, microbial biomass and mycorrhizal colonisation in upland grassland. *Plant and Soil*, *271*(1), 157–164. https://doi.org/10.1007/s11104-004-2267-z

Kuo, S. (1996). Phosphorus. In D. L. Sparks (Ed.), *Methods of Soil Analysis: Part 3*, *SSSA Book Series No. 5* (pp. 869–919). SSSA and ASA. https://doi.org/10.2136/sssabookser5.3.c32

Liu, J., Yongfeng, H., Yang, J., Abdi, D., & Cade-Menun, B. J. (2014). Investigation of soil legacy phosphorus transformation in long-term agricultural fields using sequential fractionation, P K-edge XANES and solution P NMR spectroscopy. *Environmental Science & Technology*, *49*(1), 168–176. https://doi.org/10.1021/es504420n

Margalef, O., Sardans, J., Maspons, J., Molowny-Horas, R., Fernández-Martínez, M., Janssens, I. A., Richter, A., Ciais, P., Obersteiner, M., & Peñuelas, J. (2021). The effect of global change on soil phosphatase activity. *Global Change Biology*, *27*(22), 5989–6003. https://doi.org/10.1111/gcb.15832

McKercher, R. B., & Anderson, G. (1968a). Characterization of the inositol penta- and hexaphosphate fractions of a number of Canadian and Scottish soils. *Journal of Soil Science*, *19*, 302–310. https://doi.org/10.1111/j.1365-2389.1968.tb01542.x

McKercher, R. B., & Anderson, G. (1968b). Content of inositol penta- and hexaphosphates in some Canadian soils. *Journal of Soil Science*, *19*, 47–55. https://doi.org/10.1111/j.1365-2389.1968.tb01519.x

McLaren, T. I., Smernik, R. J., McLaughlin, M. J., McBeath, T. M., Kirby, J. K., Simpson, R. J., Guppy, C. N., Doolette, A. L., & Richardson, A. E. (2015). Complex forms of soil organic phosphorus-a major component of soil phosphorus. *Agricultural Science and Technology*, *49*(22), 13238–13245. https://doi.org/10.1021/acs.est.5b02948

McLaren, T. I., Verel, R., & Frossard, E. (2022). Soil phosphomonoesters in large molecular weight material comprise multiple components. *Soil Science Society of America Journal*, *86*(2), 345–357. https://doi.org/10.1002/saj2.20347

Newman, R. H., & Tate, K. R. (1980). Soil phosphorus characterisation by 31P nuclear magnetic resonance. *Communications in Soil Science and Plant Analysis*, *11*, 835–842. https://doi.org/10.1080/00103628009367083

Papanikolaou, N., Britton, A. J., Helliwel, R. C., & Johnson, D. (2010). Nitrogen deposition, vegetation burning and climate warming act independently on microbial community structure and enzyme activity associated with decomposing litter in low-alpine heath. *Global Change Biology*, *16*(11), 3120–3132. https://doi.org/10.1111/j.1365-2486.2010.02196.x

Raboy, V. (2003). *myo*-Inositol-1,2,3,4,5,6-hexakisphosphate. *Phytochemistry*, *64*(6), 1033–1043. https://doi.org/10.1016/s0031-9422(03)00446-1

Reusser, J. E., Piccolo, A., Vinci, G., Savarese, C., Cangemi, S., Cozzolino, V., Verel, R., Frossard, E., & McLaren, T. I. (2023). Phosphorus species in sequentially extracted soil organic matter fractions. *Geoderma*, *429*, 116227. https://doi.org/10.1016/j.geoderma.2022.116227

Reusser, J. E., Verel, R., Frossard, E., & McLaren, T. I. (2020). Quantitative measures of: *Myo*-IP_6 in soil using solution 31P NMR spectroscopy and spectral deconvolution fitting including a broad signal. *Environmental Science. Processes & Impacts*, *22*, 1084–1094.

Reusser, J. E., Verel, R., Zindel, D., Frossard, E., & McLaren, T. I. (2020). Identification of lower-order inositol phosphates (IP_5 and IP_4) in soil extracts as determined by hypobromite oxidation and solution 31P NMR spectroscopy. *Biogeosciences*, *17*, 5079–5095. https://doi.org/10.5194/bg-17-5079-2020

Rugova, A., Puschenreiter, M., Santner, J., Fischer, L., Neubauer, S., Koellensperger, G., & Hann, S. (2014). Speciation analysis of orthophosphate and *myo*-inositol hexakisphosphate in soil- and

plant-related samples by high-performance ion chromatography combined with inductively coupled plasma mass spectrometry. *Magnetic Resonance in Medicine*, *37*, 1711–1719. https://doi.org/10.1002/jssc.201400026

Schreider, K., Boy, J., Sauheitl, L., Figueiredo, A. F., Andrino, A., & Guggenberger, G. (2022). Designing a robust and versatile system to investigate nutrient exchange in, and partitioning by, mycorrhiza (*Populus* x *canesces* x *Paxillus involutus*) under axenic or greenhouse conditions. *Frontiers in Fungal Biology*, *3*, 1–11. https://doi.org/10.3389/ffunb.2022.907563

Smernik, R. J., & Dougherty, W. J. (2007). Identification of phytate in phosphorus-31 nuclear magnetic resonance spectra: The need for spiking. *Soil Science Society of America Journal*, *71*, 1045–1050. https://doi.org/10.2136/sssaj2006.0295

Spohn, M. (2020). Phosphorus and carbon in soil particle size fractions: A synthesis. *Biogeochemistry*, *147*(3), 225–242. https://doi.org/10.1007/s10533-019-00633-x

Spohn, M., & Stendahl, J. (2022). Carbon, nitrogen, and phosphorus stoichiometry of organic matter in Swedish forest soils and its relationship with climate, tree species, and soil texture. *Biogeosciences*, *19*(8), 2171–2186. https://doi.org/10.5194/bg-19-2171-2022

Thomas, M. P., Mills, S. J., & Potter, B. V. L. (2016). The "other" inositols and their phosphates; synthesis, biology and medicine (with recent advances in *myo*-inositol chemistry). *Angewandte Chemie (International Ed. in English)*, *55*(5), 1614–1650. https://doi.org/10.1002/anie.201502227

Turner, B. L. (2008). Resource partitioning for soil phosphorus: A hypothesis. *Journal of Ecology*, *96*(4), 698–702. https://doi.org/10.1111/j.1365-2745.2008.01384.x

Turner, B. L., Cheesman, A. W., Godage, H. Y., Riley, A. M., & Potter, B. V. L. (2012). Determination of *neo*- and D-*chiro*-inositol hexakisphosphate in soils by solution 31P NMR spectroscopy. *Environmental Science & Technology*, *46*(9), 4994–5002. https://doi.org/10.1021/es204446z

Turner, B. L., Paphazy, M. J., Haygarth, P. M., & McKelvie, I. D. (2002). Inositol phosphates in the environment. *Philosophical Transactions of the Royal Society of London. Series B, Biological Sciences*, *357*(1420), 449–469. https://doi.org/10.1098/rstb.2001.0837

Turner, B. L., & Wright, J. S. (2014). The response of microbial biomass and hydrolytic enzymes to a decade of nitrogen, phosphorus, and potassium addition in a lowland tropical rain forest. *Biogeochemistry*, *117*(1), 115–130. https://doi.org/10.1007/s10533-013-9848-y

Vance, E. D., Brookes, P. C., & Jenkinson, D. S. (1987). An extraction method for measuring soil microbial biomass C. *Soil Biology and Biochemistry*, *19*(6), 703–707. https://doi.org/10.1016/0038-0717(87)90052-6

Whitfield, H., Riley, A. M., Diogenous, S., Godage, H. Y., Potter, B. V. L., & Brearley, C. A. (2018). Simple synthesis of (32)P-labelled inositol hexakisphosphates for study of phosphate transformations. *Plant and Soil*, *427*, 149–161. https://doi.org/10.1007/s11104-017-3315-9

Whitfield, H., White, G., Sprigg, C., Riley, A. M., Potter, B. V. L., Hemmings, A. M., & Brearley, C. A. (2020). An ATP-responsive metabolic cassette comprised of inositol tris/tetrakisphosphate kinase 1 (ITPK1) and inositol pentakisphosphate 2-kinase (IPK1) buffers diphosphosphoinositol phosphate levels. *The Biochemical Journal*, *477*, 2621–2638. https://doi.org/10.1042/BCJ20200423

SUPPORTING INFORMATION

Additional supporting information can be found online in the Supporting Information section at the end of this article.

Table S1. Soil parameters of the forest stand in Åsele, Sweden.

Table S2. Detector response to P as function of mobile phase HCl concentration.

Figure S1. Calibration of detector (S-TQ-O_2) response to injection of *myo*-InsP_6.

Figure S2. Separation and detection of inositol hexakisphosphates by LC-ICP-MS.

Figure S3. LC-ICP-MS of a diluted soil sample.

Figure S4. Separation of pyrophosphate and trimetaphosphate from inositol phosphate isomers.

Figure S5. LC-ICP-MS of extracts of single seeds of *Arabidopsis thaliana*.

How to cite this article: Carroll, J. J., Sprigg, C., Chilvers, G., Delso, I., Barker, M., Cox, F., Johnson, D., & Brearley, C. A. (2024). LC-ICP-MS analysis of inositol phosphate isomers in soil offers improved sensitivity and fine-scale mapping of inositol phosphate distribution. *Methods in Ecology and Evolution*, *15*, 530–543. https://doi.org/10.1111/2041-210X.14292